Supplementary material for

**Dysregulation of miR-219 promotes neurodegeneration through post-transcriptional regulation of tau**

Ismael Santa-Maria, Maria E. Alaniz, Neil Renwick, Carolina Cela, Tudor Fulga, David L. Van Vactor, Thomas Tuschl, Lorraine N. Clark, Michael L. Shelanski, Brian D. McCabe, John F. Crary*

*Corresponding author. E-mail: john.crary@mountsinai.org

**This file includes**

Supplementary Methods

Supplementary Figures 1 to 5

Supplementary Tables 1 to 5

Supplementary References

**Methods**

*Patient samples.* De-identified human autopsy brain tissue (Supplementary Table 1) from Broadmann area 9 was obtained from the New York Brain Bank at Columbia University, University of Kentucky (Lexington, KY, USA), the University of California San Diego (San Diego, CA, USA), the Banner Sun Health Research Institute (Sun City, AZ, USA) and the University of Washington (Seattle, WA, USA).

*RNA isolation.* Fresh-frozen brain tissue was pulverized in liquid nitrogen, lysed in QIAzol and homogenized using a QIAshredder column. Total RNA was extracted using the miRNeasy Kit (Qiagen). A subset of total RNA samples was purified using TRIzol and similar results were obtained (Life Technologies). RNA was assessed on an Agilent 2100 Bioanalyzer system using the Agilent RNA 6000 Nano Assay kit and a Nanodrop Spectrophotometer (Thermoscientific).

*Small RNA sequencing and annotation.* A barcoded small RNA cDNA library was prepared from total RNA as previously described (1). Briefly, 100 ng of total RNA from each sample was spiked with a set of synthetic calibration markers of known concentration prior to ligation to a sample-specific 3' oligonucleotide adapter. Following sample pooling, 5' adapter ligation, and reverse-transcription polymerase chain reaction amplification, the resulting complementary DNA was Illumina sequenced. Small RNA sequences were analyzed using a web-accessible graphical user interface (RNAworld.rockefeller.edu). Once the sequences were aligned to the genome (hg19) and annotations were assigned, miRNA abundance was determined as the sum of all reads with up to two annotations mismatches and normalized to read frequency. Curated definitions were used for annotation. Quantitative miRNA profiles were generated and unsupervised hierarchical clustering of samples was performed to assess sample grouping (2). Heat map generation and data analysis were performed within the R/Bioconductor statistical framework (3, 4).

*Human brain QPCR.* DNA synthesis was performed using the First Strand cDNA Synthesis Kit (Origene). QPCR was performed on a Mastercycler ep realplex (Eppendorf) using TaqMan Gene Expression Master Mix and

primers and TaqMan probes specific for total tau and GAPDH mRNAs (Life Technologies). The following settings were used: 95 °C for 10 min followed by 40 cycles of 95 °C for 15 s and 60 °C for 1 min. The GAPDH mRNA levels were used for normalization. TaqMan MicroRNA assays were used to measure miR-219-5p levels (Life Technologies). 100 ng of total RNA was reverse-transcribed using specific stem-loop reverse transcription primers (Life Technologies) and miR-219-5p levels were measured on a Mastercycler ep realplex (Eppendorf). The levels of U24/SNORD24 and Z30/SNORD7 were used as endogenous controls for normalization using the comparative CT method.

*Target prediction.* Currently, integration of various computational methods is a common approach to improve prediction accuracy and to create an optimal framework for deciphering biological functions of miRNAs (5). We used TargetScan (6) and miRBase (7) to identify miRNAs that are predicted to bind the tau 3' UTR. TargetScan is a well-established algorithm of seed and sequence complementarity with conservation of binding sites across multiple species that has been shown to result in the most accurate predictions upon target validation (8, 9).

*Drosophila strains*. *Drosophila* miR-219 or scrambled control lines (a generous gift from Eric C. Lai, Memorial Sloan-Kettering Cancer Center, NY) were derived from a UAS-DsRed-miRNA plasmid collection (10). The miRNA inserts included ~200-250 nucleotides flanking each side of the pre-miRNA hairpin and were amplified from $w^{1118}$ or Canton S genomic DNA. To generate *Drosophila* miRNA sponge or scrambled controls, ten repetitive sequences complementary to a miRNA with mismatches at positions 9–12 for enhanced stability were introduced into the 3′ UTR of *EGFP* or *mCherry* in a pUAST expression vector (11). We generated transgenic *Drosophila* lines that express the luciferase coding region fused with either a control GAPDH 3' UTR or the full-length human tau 3' UTR (see below) using a series of *Drosophila* phiC31 compatible GAL4-UAS vectors termed pBID (attB, Insulated, *Drosophila*) (12). For tau overexpression, we also used the pBID system with the full-length human tau coding sequence (2N4R). For pan-neuronal expression, the *elav-GAL4* driver was used. The GMR-GAL4 driver for expression of transgenes in the eye. All *Drosophila* crosses were maintained at 25 °C.

*Drosophila rough eye phenotypic scoring*. Eye phenotypes were recorded from 2 day old adult *Drosophila* and scored, in a blinded fashion, by three independent observers as descried by others with modifications (13). Semi-quantitative assessment of the rough eye phenotypes was achieved in the following way: specified genotypes were collected and recorded under a dissecting microscope by one researcher, coded and given to another three researchers for blind scoring. Recorded images of 'Test' *Drosophila* eyes were viewed and each individual fly was given a relative roughness score in comparison with the known scoring classes (Supplementary Figure 4): (1) Slightly rough; greater degree of organization; ommatidia malformed, least reduction in eye size. (2) Rough; less degree of organization; ommatidia malformed and slightly fused; reduced in size. (3) Rougher; loss of organization; ommatidia malformed and fused; more pronounced reduction in size. (4) Roughest; complete loss of organization; eye lacks a recognizable morphology, and pronounced invaginations on the eye surface; marked reduction in size. Scores were collected for 38 individual flies per group before the blinding was removed.

*Drosophila immunoblotting*. Adult flies were homogenized in Neuronal Protein Extraction Reagent supplemented with Halt Protease & Phosphatase inhibitor cocktail (Thermo Scientific). Lysates were incubated on ice for 10 min and centrifuged at 13,000 x *g* for 15 min at 4 °C. Protein concentration was determined using the BCA protein assay (Thermo Scientific). Samples were resolved by SDS-PAGE and analyzed by immunoblot as previously described (14) with antisera targeting *Drosophila* tau (a gift from Dr. Nick Lowe, University of Cambridge, UK) or β-actin (Sigma-Aldrich).

*Drosophila luciferase reporter assay*. *Drosophila* luciferase reporter lines were crossed with either the miR-219 or the miR-219 sponge lines or their respective controls. The pan-neuronal *elav-GAL4* driver was used to drive transgene expression. Luciferase activity was measured from the lysate of pooled adult *Drosophila* heads using the Luciferase Reporter Assay System (Promega). A control line with a GAPDH 3' UTR was used for normalization.

*Drosophila QPCR*. Total RNA was isolated from the whole *Drosophila*. Briefly, flies were lysed in QIAzol and homogenized using a QIAshredder column. Total RNA was extracted using the miRNeasy Kit (Qiagen). RNA concentrations were measured with a Nanodrop ND-1000 Spectrophotometer. Equal amounts of RNA were reverse transcribed using the First Strand cDNA Synthesis Kit (Origene) according to the manufacturer's instructions. QPCR for *Drosophila* tau and the endogenous control RpL32 was performed using TaqMan Gene Expression assays (Life Technologies). Real-time PCR reactions were performed in triplicate with MicroAmp optical 96-well plates using a Mastercycler ep realplex (Eppendorf) with the following conditions; an initial step of 10 min at 95 °C, followed by 40 cycles of 15 s at 95 °C, 1 min at 60 °C. TaqMan MicroRNA assays were used to measure miR-219-5p levels (Life Technologies). Total RNA was reverse-transcribed using specific stem-loop reverse transcription primers (Life Technologies) and miR-219-5p levels were measured with TaqMan MicroRNA assays on a Mastercycler ep realplex (Eppendorf). The levels of 2srRNA were used as endogenous control for normalization using the comparative CT method. Each data point is the result of at least three biological replicates each composed of three technical replicates.

*Plasmids*. The full-length human *MAPT* 3' UTR was amplified from genomic DNA from a control subject using the following primers F: 5'-AATTCTAGGCGATCGCTCGAGAAGCAGGGTTTGTGATCAGG-3' and R: 5'-ATTTTATTGCGGCCAGCGGCCGCGGTGCGTGGGAAAGAACTTA-3' and cloned between the XhoI and NotI sites of the dual-luciferase reporter psiCHECK-2 vector (Promega) using the In-Fusion HD cloning kit (Clontech/Takara Bio Inc.). This quantitative system utilizes a primary *Renilla* luciferase reporter and a secondary firefly luciferase reporter expression cassette for normalization, which controls for transfection efficiency and cell death. Site-directed mutagenesis of the miR-219 recognition element was performed using the QuickChange II XL Site-Directed Mutagenesis Kit (Agilent). Primers, generated using QuickChange Primer Design, were F: 5'-C ACGCTGGCTTGTGATCTTAAATGAGGGTCGATCCCCCAGGGCTGGGCACTC-3' and R: 5'-GAGTGCCC AGCCCTGGGGGATCGACCCTCATTTAAGATCACAAGCCAGCGTG-3'. Sequences were verified by Sanger sequencing.

*Lentiviral vectors.* The human mir-219 precursor and the scrambled miRNA control were obtained from Genecopoeia. Lentiviral production was performed as described by others (15). We used the human HEK 293T cell line for optimal lentivirus production. HEK 293T cells (ATCC) were grown either in Dulbecco's modified Eagle's medium (DMEM) or DMEM/F12 medium (Cellgro) supplemented with 10% fetal bovine serum, 2 mM glutamine, 100 units/ml penicillin, and 100 μg/ml streptomycin in a humidified atmosphere of 5% CO2 and 95% air at 37 °C. Lentiviral stock titration was carried out using the Global UltraRapid Lentiviral Titer Kit (System Biosciences).

*Cell culture.* Human neuroblastoma SH-SY5Y cells (ATCC) were grown either in DMEM or DMEM/F12 medium (Cellgro) supplemented as mentioned above for HEK 293T cells. PC12 cells were cultured as described previously by others in collagen-coated dishes with RPMI 1640 medium supplemented with 10% heat-inactivated horse serum and 5% FBS (16). Neuronal differentiation media for PC12 contains: NGF (100 ng of human recombinant protein per ml) and RPMI 1640 medium supplemented with 1% heat-inactivated donor horse serum.

*Luciferase assays.* SH-SY5Y neuroblastoma cells were plated at a density of $8\times10^4$ cells per well (in 24-well plates) 24 hr before transfection. Luciferase reporter constructs were cotransfected with miRNA mirVana mimics (Ambion) using Lipofectamine 2000 (Life Technologies). Firefly and *Renilla* luciferase activities were measured 48 hr after transfection using the dual-luciferase reporter assay system (Promega). At least six transfection assays were performed for each condition.

*Immunocytochemistry.* PC12 cells were fixed with 4.0% paraformaldehyde (Thermo Scientific) and permeabilized with 0.4% Triton X-100 (Sigma-Aldrich, St. Louis, MO) in PBS, blocked with SuperBlock buffer in TBS (Thermo Scientific) and incubated overnight in the TauC antisera (DAKO). Anti-mouse secondary antisera conjugated with Alexa Fluor dyes (Life Technologies) were used. Labeled PC12 cells or neurons were imaged using an AxioObserver Z1 microscope and the imaging software Axiovision Rel 4.8.2 (Carl Zeiss).

*Immunoblotting of mammalian cell extracts.* Total protein was resolved by sodium dodecyl sulphate-polyacrylamide gel electrophoresis (SDS-PAGE) and transblotted using standard procedures. Nitrocellulose membranes (BioRad) were incubated with TauC (DAKO), β-actin (Sigma-Aldrich) and secondary antibodies (Thermo Fisher Scientific), and revealed by chemiluminescence using the ECL kit (Millipore) and Biomax Light films (Sigma-Aldrich).

**Supplementary Figures**

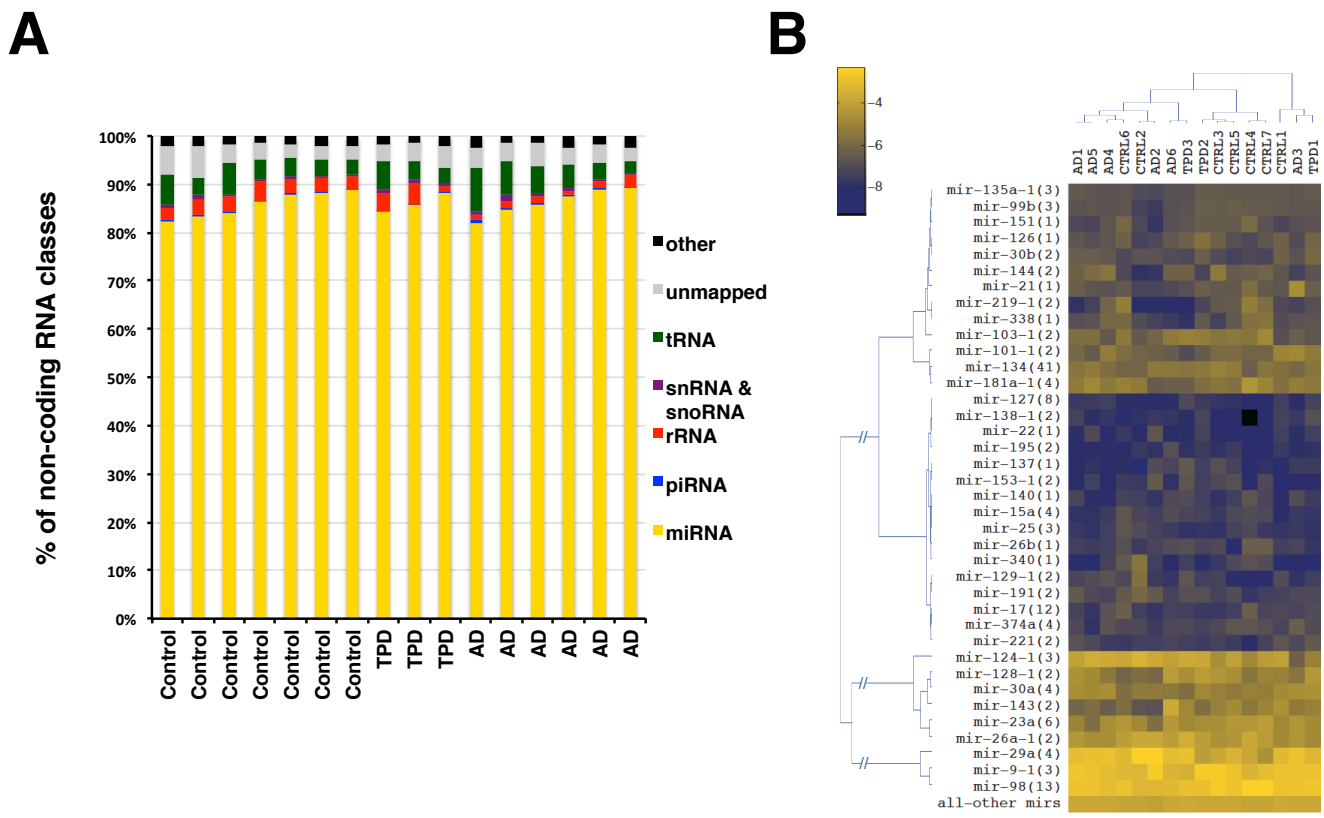


**Supplementary Figure 1**

Small RNA sequencing. (**A**) Histogram showing the proportion of reads mapping to non-coding RNA subgroups. (**B**) Heat map diagram with unsupervised hierarchical clustering of miRNA changes in Alzheimer's disease (AD)(*n*=6), tangle predominant dementia (TPD) (*n*=3) and control (*n*=7). Data are shown as a pseudo-colored heat map ($log_2$ transformed relative expression values of the normalized read frequency).

**A**

***Homo sapiens (hsa) mir-219***

**mir-219-1 DNA sequence** (chr6: 33175612-33175721):

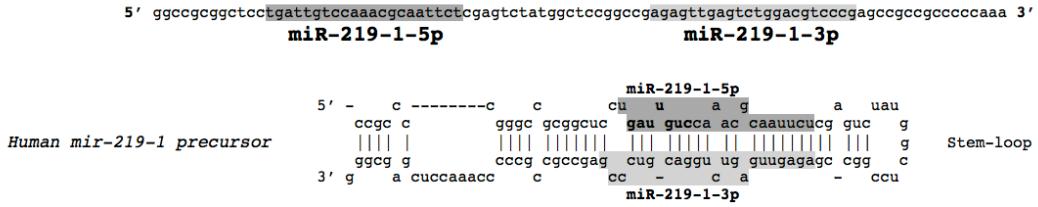


**mir-219-2 DNA sequence** (chr9: 131154900-131154987):

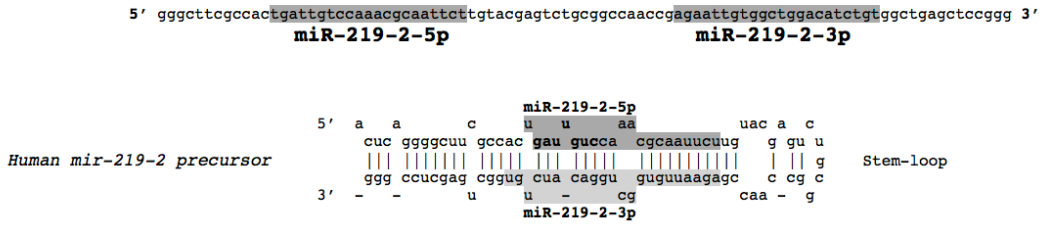


**B**

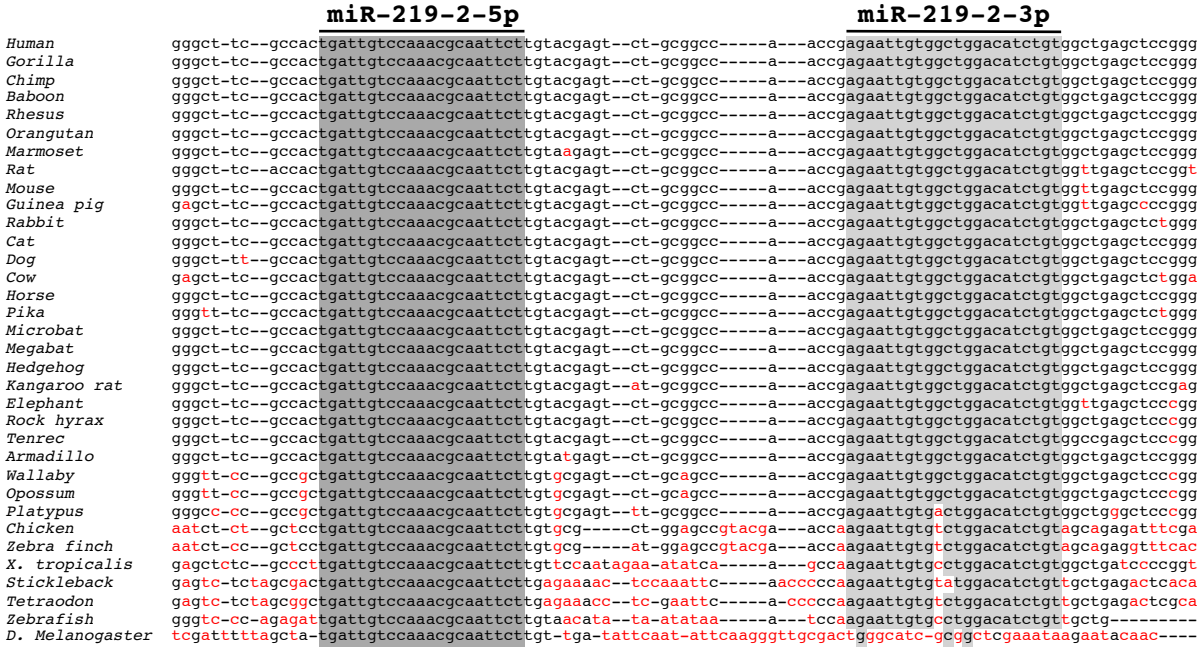


**Supplementary Figure 2**

Structure of mir-219 and conservation of miR-219-5p (miR-219). (**A**) Human mir-219-1 and mir-219-2 precursor stem loop structures. (**B**) Sequence alignment illustrates a high degree of evolutionary conservation of the mature miRNAs.

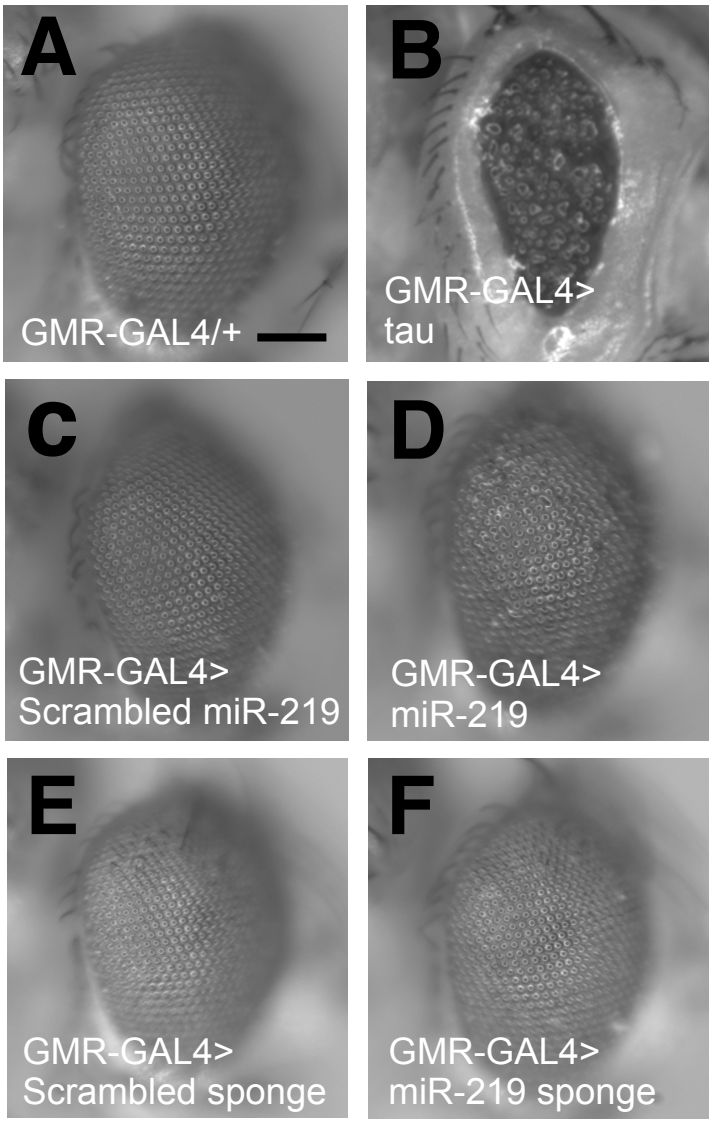


**Supplementary Figure 3**

*Drosophila* rough eye phenotypes.

(**A**) Adult transgenic animals expressing the GMR-GAL4 eye driver alone display a normal ommatidial lattice. (**B**) A severe rough eye phenotype, with markedly reduced eye size and irregular ommatidial structure, is generated by expression of UAS-tau (human) using the GMR-GAL4 driver. (**C**, **D**) Expression of miR-219 using the GMR-GAL4 driver induces a very mild rough eye phenotype as compared to the scrambled miR-219 control line. (**E**, **F**) Neither expression of the miR-219 sponge nor the scrambled sponge induce a rough eye phenotype. Bar in (**A**-**F**), 100 μm.

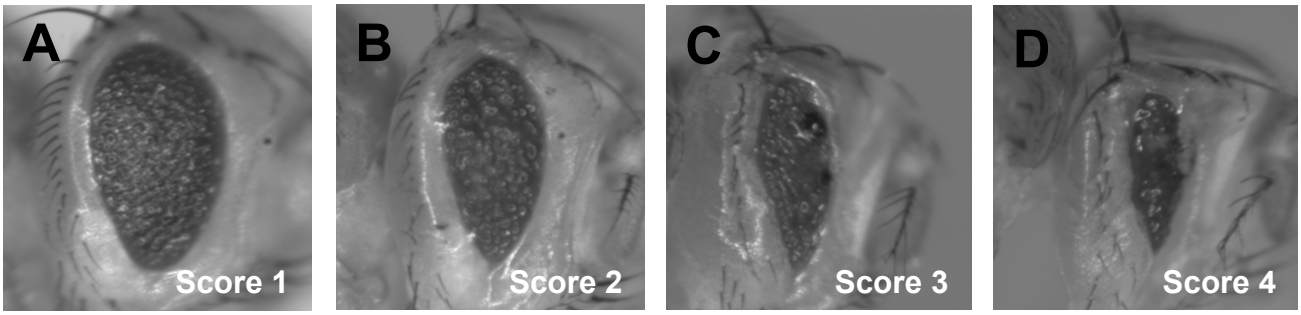


**Supplementary Figure 4**

*Drosophila* rough eye scoring.

(**A-D**) Representative light microscopic images illustrating the categories used for semi-quantitative scoring of the rough eye severity (see Supplementary Methods).

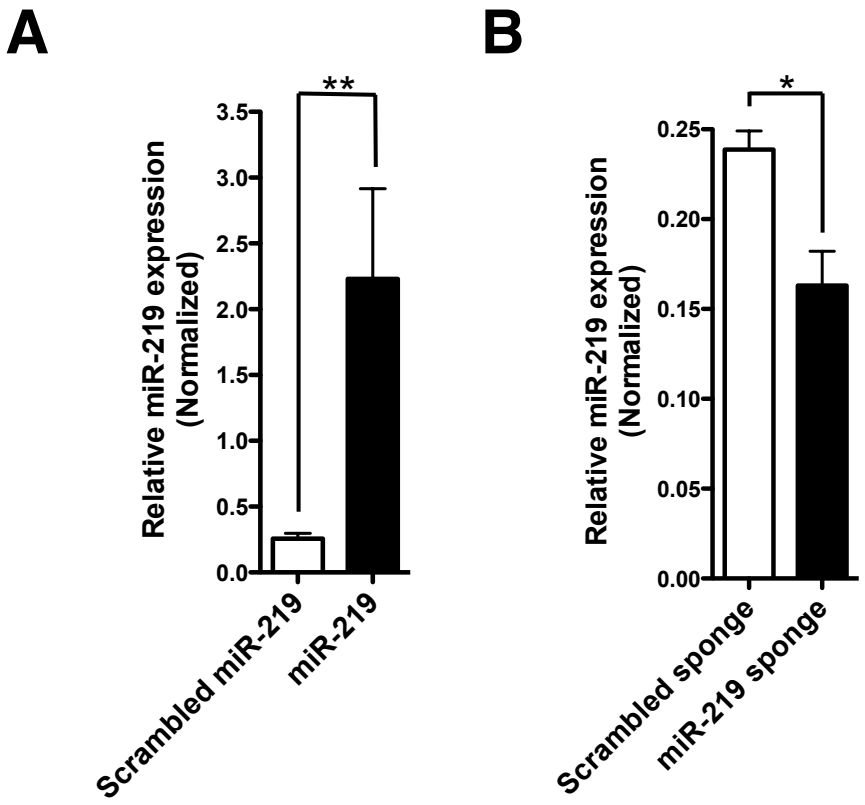


**Supplementary Figure 5**

Experimental manipulation of miR-219 levels in *Drosophila*. (**A**) Real-time miRNA-PCR of flies expressing miR-219 show a significant 8.7 fold increase in miR-219 levels compared to controls (normalized to 2sRNA). (**B**) The miR-219 sponge significantly reduces the endogenous *Drosophila* miR-219 levels compared to controls. Data are means ± SEM and representative of $n$=3 experiments. Statistical analysis was performed using a Student's t-test (two-tailed distribution, *$P \leq 0.05$, **$P \leq 0.01$).

**Supplementary Tables**

**Supplementary Table 1.** Summary of patient data

| Classification | *n* | Sex (M/F) | Average age (yr ± SEM) | Braak NFT | Limbic NFT Frequency | CERAD plaque score | Clinical diagnosis |
|---|---|---|---|---|---|---|---|
| Control | 20 | 9/11 | 89 ± 4.5 | 0-IV | Sparse | 0-A | Normal |
| TPD | 21 | 4/17 | 89 ± 3.4 | III-IV | Frequent | 0-A | AD or MCI |
| AD | 7 | 3/4 | 93 ± 3.9 | V-VI | Frequent | B-C | AD |

SEM = standard error of the mean; AD = Alzheimer's disease; TPD = tangle-predominant dementia; MCI = mild cognitive impairment; CERAD plaque score 0 = none, A = sparse, B = moderate, C = frequent

**Supplementary Table 2.** Small RNA sequencing summary statistics in AD, TPD and control

| | | Total | miRNA | | None | | rRNA | | tRNA | | Other RNA | | Marker | |
|---|---|---|---|---|---|---|---|---|---|---|---|---|---|---|
| **Case** | **Classification** | **Reads** | **Reads** | **%** | **Reads** | **%** | **Reads** | **%** | **Reads** | **%** | **Reads** | **%** | **Reads** | **%** |
| 1 | AD | 16,013,090 | 13,516,502 | 84.4% | 631,838 | 3.9% | 216,699 | 1.4% | 1,071,952 | 6.7% | 359,765 | 2.2% | 3,435 | 0.02% |
| 2 | AD | 6,964,402 | 6,261,001 | 89.9% | 182,352 | 2.6% | 184,355 | 2.6% | 186,129 | 2.7% | 53,915 | 0.8% | 1,809 | 0.03% |
| 3 | AD | 13,401,542 | 11,839,644 | 88.3% | 490,613 | 3.7% | 140,233 | 1.0% | 647,086 | 4.8% | 127,928 | 1.0% | 4,356 | 0.03% |
| 4 | AD | 11,848,169 | 10,565,866 | 89.2% | 445,991 | 3.8% | 162,432 | 1.4% | 419,594 | 3.5% | 109,690 | 0.9% | 4,166 | 0.04% |
| 5 | AD | 5,515,061 | 4,552,854 | 82.6% | 232,377 | 4.2% | 60,701 | 1.1% | 510,384 | 9.3% | 74,651 | 1.4% | 1,109 | 0.02% |
| 6 | AD | 10,955,968 | 9,321,534 | 85.1% | 546,730 | 5.0% | 148,371 | 1.4% | 592,747 | 5.4% | 142,417 | 1.3% | 3,821 | 0.03% |
| 7 | TPD | 7,358,781 | 6,254,750 | 85.0% | 267,537 | 3.6% | 313,761 | 4.3% | 271,358 | 3.7% | 100,916 | 1.4% | 6,708 | 0.09% |
| 8 | TPD | 46,009,737 | 40,915,306 | 88.9% | 2,178,534 | 4.7% | 582,308 | 1.3% | 1,424,294 | 3.1% | 349,222 | 0.8% | 6,140 | 0.01% |
| 9 | TPD | 11,761,875 | 9,848,425 | 83.7% | 409,442 | 3.5% | 434,062 | 3.7% | 708,530 | 6.0% | 118,867 | 1.0% | 4,886 | 0.04% |
| 10 | Control | 6,965,614 | 5,822,543 | 83.6% | 257,263 | 3.7% | 222,735 | 3.2% | 446,921 | 6.4% | 60,513 | 0.9% | 2,390 | 0.03% |
| 11 | Control | 8,642,905 | 7,708,564 | 89.2% | 228,211 | 2.6% | 229,337 | 2.7% | 274,206 | 3.2% | 59,315 | 0.7% | 9,961 | 0.12% |
| 12 | Control | 9,460,257 | 8,382,841 | 88.6% | 244,563 | 2.6% | 251,069 | 2.7% | 339,873 | 3.6% | 100,199 | 1.1% | 5,051 | 0.05% |
| 13 | Control | 8,041,382 | 7,043,196 | 87.6% | 231,342 | 2.9% | 227,777 | 2.8% | 320,541 | 4.0% | 75,385 | 0.9% | 2,579 | 0.03% |
| 14 | Control | 47,219,748 | 38,939,377 | 82.5% | 2,720,085 | 5.8% | 1,141,842 | 2.4% | 2,974,965 | 6.3% | 491,026 | 1.0% | 6,035 | 0.01% |
| 15 | Control | 10,182,030 | 8,722,291 | 85.7% | 348,294 | 3.4% | 394,717 | 3.9% | 410,679 | 4.0% | 108,940 | 1.1% | 4,951 | 0.05% |
| 16 | Control | 5,517,456 | 4,581,894 | 83.0% | 365,643 | 6.6% | 179,489 | 3.3% | 195,525 | 3.5% | 70,389 | 1.3% | 644 | 0.01% |

AD = Alzheimer's disease; TPD = tangle-predominant dementia; other RNA = piRNA, snRNA and snoRNA

**Supplementary Table 3.** Comparison of mir-219 read frequencies in AD, TPD and control

| | | miR-219-5p | | miR-219-1-3p | | miR-219-2-3p | |
|---|---|---|---|---|---|---|---|
| **Case** | **Classification** | **Reads** | **%** | **Reads** | **%** | **Reads** | **%** |
| 1 | AD | 183,085 | 1.35% | 1 | 0.00% | 11,165 | 0.08% |
| 2 | AD | 14,303 | 0.23% | 1 | 0.00% | 8,118 | 0.13% |
| 3 | AD | 48,438 | 0.41% | 6 | 0.00% | 26,038 | 0.22% |
| 4 | AD | 50,131 | 0.48% | 1 | 0.00% | 17,342 | 0.16% |
| 5 | AD | 13,928 | 0.31% | 3 | 0.00% | 5,127 | 0.11% |
| 6 | AD | 28,084 | 0.30% | 3 | 0.00% | 14,228 | 0.15% |
| 7 | TPD | 25,975 | 0.41% | 2 | 0.00% | 18,523 | 0.30% |
| 8 | TPD | 228,931 | 0.55% | 10 | 0.00% | 140,699 | 0.34% |
| 9 | TPD | 21,249 | 0.21% | 3 | 0.00% | 9,631 | 0.10% |
| 10 | Control | 121,194 | 2.08% | 1 | 0.00% | 33,834 | 0.58% |
| 11 | Control | 77,222 | 1.00% | 2 | 0.00% | 72,402 | 0.94% |
| 12 | Control | 57,114 | 0.68% | 1 | 0.00% | 39,576 | 0.47% |
| 13 | Control | 119,188 | 1.70% | 5 | 0.00% | 77,779 | 1.10% |
| 14 | Control | 217,944 | 0.56% | 8 | 0.00% | 81,925 | 0.21% |
| 15 | Control | 47,953 | 0.55% | 2 | 0.00% | 49,236 | 0.56% |
| 16 | Control | 11,494 | 0.25% | 2 | 0.00% | 6,489 | 0.14% |

AD = Alzheimer's disease; TPD = tangle-predominant dementia

**Supplementary Table 4.** Predicted miRNA recognition elements in the *Drosophila* tau 3' untranslated region (UTR)

| miRNA family | Site type | 3' UTR start | 3' UTR end |
|---|---|---|---|
| miR-980 | 7mer-1a | 90 | 96 |
| miR-33 | 8mer | 129 | 135 |
| miR-954 | 8mer | 164 | 170 |
| miR-193 | 7mer-1a | 182 | 188 |
| miR-1012 | 7mer-m8 | 304 | 310 |
| miR-33 | 7mer-m8 | 317 | 323 |
| miR-977 | 8mer | 356 | 362 |
| miR-967 | 7mer-1a | 357 | 363 |
| miR-33 | 7mer-1a | 534 | 540 |
| miR-3/309/318 | 7mer-1a | 561 | 567 |
| miR-219 | 8mer | 864 | 870 |
| miR-315 | 7mer-m8 | 867 | 873 |
| miR-966 | 7mer-1a | 889 | 895 |
| miR-961 | 7mer-m8 | 1015 | 1021 |
| miR-281-2-3p | 7mer-1a | 1056 | 1062 |
| miR-959 | 7mer-1a | 1056 | 1062 |
| miR-8 | 7mer-m8 | 1136 | 1142 |
| miR-184 | 7mer-1a | 1293 | 1299 |
| miR-927 | 7mer-1a | 1421 | 1427 |
| miR-277 | 7mer-1a | 1496 | 1502 |
| miR-1000 | 7mer-1a | 1510 | 1516 |
| miR-210.1 | 7mer-1a | 1542 | 1548 |

TargetScan predicts the following site types: 8mer: an exact match to positions 2-8 of the mature miRNA (the seed + position 8) followed by an 'A'. 7mer-m8: an exact match to positions 2-8 of the mature miRNA (the seed + position 8). 7mer-1a: an exact match to positions 2-8 of the mature miRNA (the seed) followed by an 'A' (17).

| Supplementary Table 5. Functional trend analysis of predicted miR-219 targets* | | |
|---|---|---|
| **Overrepresented attributes** | | |
| **Gene Ontology ID** | **Name** | ***p* (adjusted)** |
| GO:0010628 | positive regulation of gene expression | <0.001 |
| GO:0022008 | neurogenesis | <0.001 |
| GO:0030182 | neuron differentiation | <0.001 |
| GO:0031175 | neuron projection development | <0.001 |
| GO:0048666 | neuron development | <0.001 |
| GO:0061564 | axon development | 0.042 |
| GO:0007399 | nervous system development | 0.004 |

*Trend analysis preformed using FuncAssociate 2.0 (18) on predicted miR-219 targets using TargetScan 6.2 (17).

**Supplementary References**


1. Hafner, M., Renwick, N., Brown, M., Mihailovic, A., Holoch, D., Lin, C., Pena, J.T., Nusbaum, J.D., Morozov, P., Ludwig, J., et al. RNA-ligase-dependent biases in miRNA representation in deep-sequenced small RNA cDNA libraries. *RNA*. 2011; 17(9):1697-1712.
2. Berninger, P., Gaidatzis, D., van Nimwegen, E., and Zavolan, M. Computational analysis of small RNA cloning data. *Methods*. 2008; 44(1):13-21.
3. Gentleman, R.C., Carey, V.J., Bates, D.M., Bolstad, B., Dettling, M., Dudoit, S., Ellis, B., Gautier, L., Ge, Y., Gentry, J., et al. Bioconductor: open software development for computational biology and bioinformatics. *Genome Biol*. 2004; 5(10):R80.
4. Anders, S., and Huber, W. Differential expression analysis for sequence count data. *Genome Biol*. 2010; 11(10):R106.
5. Zhang, Y., and Verbeek, F.J. Comparison and integration of target prediction algorithms for microRNA studies. *J Integr Bioinform*. 2010; 7(3).
6. Lewis, B.P., Burge, C.B., and Bartel, D.P. Conserved seed pairing, often flanked by adenosines, indicates that thousands of human genes are microRNA targets. *Cell*. 2005; 120(1):15-20.
7. Griffiths-Jones, S. The microRNA Registry. *Nucleic Acids Res*. 2004; 32(Database issue):D109-111.
8. Baek, D., Villen, J., Shin, C., Camargo, F.D., Gygi, S.P., and Bartel, D.P. The impact of microRNAs on protein output. *Nature*. 2008; 455(7209):64-71.
9. Selbach, M., Schwanhausser, B., Thierfelder, N., Fang, Z., Khanin, R., and Rajewsky, N. Widespread changes in protein synthesis induced by microRNAs. *Nature*. 2008; 455(7209):58-63.

10. Bejarano, F., Bortolamiol-Becet, D., Dai, Q., Sun, K., Saj, A., Chou, Y.T., Raleigh, D.R., Kim, K., Ni, J.Q., Duan, H., et al. A genome-wide transgenic resource for conditional expression of Drosophila microRNAs. *Development*. 2012; 139(15):2821-2831.

11. Loya, C.M., Lu, C.S., Van Vactor, D., and Fulga, T.A. Transgenic microRNA inhibition with spatiotemporal specificity in intact organisms. *Nat Methods*. 2009; 6(12):897-903.

12. Wang, J.W., Beck, E.S., and McCabe, B.D. A modular toolset for recombination transgenesis and neurogenetic analysis of Drosophila. *PLoS One*. 2012; 7(7):e42102.

13. Reid, D.W., Muyskens, J.B., Neal, J.T., Gaddini, G.W., Cho, L.Y., Wandler, A.M., Botham, C.M., and Guillemin, K. Identification of genetic modifiers of CagA-induced epithelial disruption in Drosophila. *Front Cell Infect Microbiol*. 2012; 2(24)1-10.

14. Santa-Maria, I., Haggiagi, A., Liu, X., Wasserscheid, J., Nelson, P.T., Dewar, K., Clark, L.N., and Crary, J.F. The MAPT H1 haplotype is associated with tangle-predominant dementia. *Acta Neuropathol*. 2012; 124(5):693-704.

15. Follenzi, A., and Naldini, L. HIV-based vectors. Preparation and use. *Methods Mol Med*. 2002; 69(259-274.

16. Greene, L.A., and Tischler, A.S. Establishment of a noradrenergic clonal line of rat adrenal pheochromocytoma cells which respond to nerve growth factor. *Proc Natl Acad Sci U S A*. 1976; 73(7):2424-2428.

17. Friedman, R.C., Farh, K.K., Burge, C.B., and Bartel, D.P. Most mammalian mRNAs are conserved targets of microRNAs. *Genome Res*. 2009; 19(1):92-105.

18. Berriz, G.F., Beaver, J.E., Cenik, C., Tasan, M., and Roth, F.P. Next generation software for functional trend analysis. *Bioinformatics*. 2009; 25(22):3043-3044.